Optics Communications 474 (2020) 126162

Contents lists available at ScienceDirect

Optics Communications

journal homepage: www.elsevier.com/locate/optcom

Research on compensating stitching testing for convex aspherical surface

Lisong Yan [a], Deyan Zhu [b], Ming Li [d], Xiaokun Wang [c], Donglin Ma [a,*]

[a] School of Optical and Electronic Information and Wuhan National Laboratory for Optoelectronics, Huazhong University of Science and Technology, Wuhan, 430074, China
[b] Nanjing University of Aeronautics and Astronautics, Nanjing, Jiangsu, 210000, China
[c] Key Laboratory of Optical System Advanced Manufacturing Technology, Changchun Institute of Optics, Fine Mechanics and Physics, Chinese Academy of Sciences, Changchun, 130033, China
[d] Intane optics, Nanjing, 210046, China

ARTICLE INFO

Keywords:
Compensating
Stitching
Convex aspherical surface
Interferometry

ABSTRACT

Aspherical optical elements bring much benefit to modern optical systems, due to its significant role in improving optical performance by compensating residual aberrations, and decreasing system's weight. However, manufacturing aspherical surfaces in high accuracy is usually limited by the ability of surface metrology, especially for convex aspherical surfaces. In this paper, we propose a compensating stitching method combining computer generated hologram (CGH) compensating testing and stitching testing to achieve the full aperture map of convex aspherical surfaces. Firstly, we introduce our self-developed mathematical models in the compensating stitching method, including CGH design model, subapertures' alignment model and stitching model. Then the performance of our proposed method is demonstrated with compensating stitching testing of an off-axis convex aspherical mirror with its aperture of 332mm×144mm. The experimental result shows that the convex aspherical surface can be tested in full aperture with our proposed method effectively, which demonstrates that our proposed surface testing method opens a new path for the testing of convex aspherical surfaces.

1. Introduction

It is always challenging to test large convex aspheric surfaces such as secondary mirrors in telescope systems by interferometry. In general, any large concave surface can be measured in full aperture with a spherical wavefront as the reference. However, it could be rather challenging to test a large flat or convex surface, because we need a reference surface in high accuracy with its aperture several times larger than the measured surface. As the aperture of secondary mirrors gets larger and larger, the full aperture test is simply impossible. A feasible alternative to tackle with the issue is subaperture stitching testing (SST). For the SST, the surface can be tested in subapertures, and each subaperture in convex surfaces can be measured to high accuracy with a small reference surface. Then the full aperture map can be obtained by combining multiple overlapping measurements with relative stitching algorithms.

SST was firstly proposed in 1980s [1–3]. According to the different shapes of subapertures, annular subaperture and circular subaperture were developed. For the annular subaperture testing, it applies only to rotational symmetric concave aspheric surfaces [4–6]. Besides the rotational symmetric concave aspheric surfaces, the circular subaperture testing can be also applied in testing the convex aspherical and freeform surfaces [7–10]. Apparently, the stitching algorithm played a vital role in the high precision stitching method. Scholars have proposed many landmark algorithms [11–15]. Obvious contributive research work includes the Kwon–Thunen method [16], the simultaneous fit method [17], the discrete phase method [18], the maximum likelihood algorithm [19,20] and the QED's variable optical null technique [21, 22].

In this paper, we focus on a compensating stitching testing method combining stitching and CGH compensating to accomplish the full aperture testing of the convex aspherical surface. Considering the fact that the departure between the convex aspherical surface and its best-fit sphere is so large that it is difficult to complete the testing simply by stitching measurement, we arranged different subaperture regions for the test surface and designed relative CGH for each subaperture. In each subaperture, null testing is conducted. Our proposed method provides an effective way to accomplish the full aperture testing of convex aspherical surfaces, especially for high-departure convex aspheres. The paper is organized as follows. In Section 2, we introduce the basic theory of our compensating stitching method. In Section 3, we present the experiment verification with our proposed method. The conclusion is given in Section 4.

* Corresponding author.
E-mail addresses: yanlisong1988@163.com (L. Yan), madonglin@hust.edu.cn (D. Ma).

https://doi.org/10.1016/j.optcom.2020.126162
Received 16 April 2020; Received in revised form 27 May 2020; Accepted 3 June 2020
Available online 6 June 2020

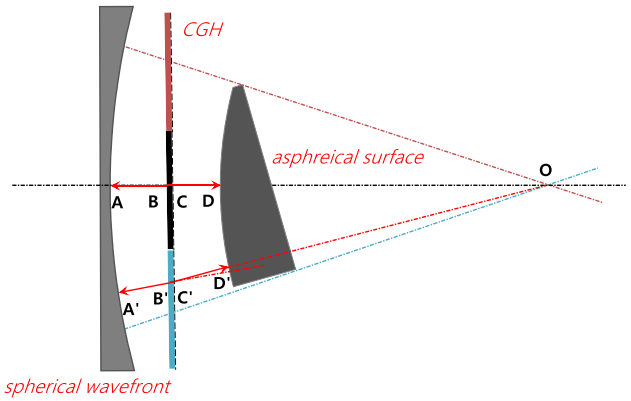

Fig. 1. Testing of aspherical surface in full aperture.

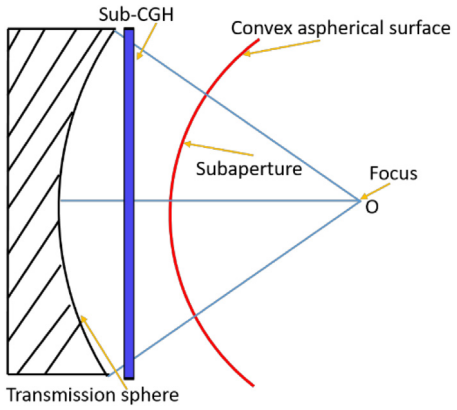

Fig. 2. Transmission sphere selection.

2. Theory

In this part, the design concept of compensating stitching testing method, including the CGH design of subapertures and alignment design between subapertures, are described in Section 2.1. Then the relative stitching algorithm are studied in Section 2.2.

2.1. Design concept of compensating stitching testing

2.1.1. CGH design of subapertures

Theoretically, a convex aspherical surface can be tested in full aperture with a CGH in larger aperture as shown in Fig. 1. The interferometer emits a spherical wavefront, which passes through CGH and accomplishes the null testing of aspherical surface in full aperture.

For the CGH, the phase distribution of aspherical compensation region can be described as follows:

$$\Delta\varphi_{main} = \frac{2\pi}{\lambda} \cdot \left[\left(A'B' + n \cdot B'C' + C'D'\right) - \left(AB + n \cdot BC + CD\right)\right] \tag{1}$$

where n is the refractive index of CGH and λ is the wavefront of light from interferometer; O is the focus point of the interferometer; A, B, C and D represent the intersection point between the chief ray and the reference surface of the interferometer, the front surface of the CGH, the rear surface of the CGH, the convex aspherical surface respectively. And A', B', C' and D' represent the intersection point between the marginal ray from the testing interferometer and the reference surface of the interferometer, the front surface of the CGH, the rear surface of the CGH, and the convex aspherical surface respectively. $A'B'$, $B'C'$, $C'D'$, AB, BC, and CD represent the distance between two corresponding points.

For the phase distribution of the alignment region between the interferometer and the CGH, it can be expressed as follows:

$$\Delta\varphi_{\text{align}} = \frac{2\pi}{\lambda} \cdot 2 \cdot \left[\left(A'B' + n \cdot B'C'\right) - \left(AB + n \cdot BC\right)\right] \tag{2}$$

As the phase distribution of aspherical surface itself is known, the phase distribution of the CGH can be calculated with ray tracing method according to the above theory accurately. However, limited by the actual aperture of the CGH, full aperture coverage of the aspherical surface is difficult to be achieved with only one CGH. To overcome the limitation, subaperture testing can be introduced. The full aperture CGH can be divided into several parts as labeled in red, black and blue color in Fig. 1. Then subaperture testing can be conducted with several pieces of CGH.

When we take subaperture testing, the standard transmission sphere should be picked first. For the testing subaperture, the aperture of CGH is D and the distance from the focus to CGH is R. The aperture of the transmission sphere is D_1, and the focus length of it is f, as shown in Fig. 2.

Table 1
Summary of CGH regions.

Region number	Function of the region
Region 1	Compensation region: Accomplish the compensation of aspherical wavefront
Region 2	Alignment region: Accomplish the alignment between CGH and interferometer
Region 3	Alignment region: Accomplish the alignment between CGH and auxiliary flat mirror

Then the transmission sphere should meet

$$\begin{cases} f > R \\ F < \frac{R}{D} \end{cases} \tag{3}$$

where $F = \frac{f}{D_1}$ is the F number of the transmission sphere. For each subaperture, the aspherical surface is null tested.

In the design of CGH, different diffraction orders should be separated. To insure orders can be eliminated in the Fourier plane by spatial filtering, wavefront tilt is added to the reference beam. Usually it requires three times the maximum wavefront slope of the surface under test to separate the first and second orders [23].

Then alignment between subapertures can be achieved with our proposed method introduced in Section 2.1.2 and the relative stitching algorithm is explained in detail in Section 2.2.

2.1.2. Alignment design

Since subaperture testing is adopted to realize the full aperture coverage of the aspherical surface, the non-alignment between subapertures will introduce extra errors in the stitching result. As a result, alignment between subapertures should be conducted accurately. To achieve this goal, three kinds of diffractive region including two alignment regions are designed on each CGH as shown in Table 1, and an auxiliary flat mirror is introduced in the subaperture testing as shown in Fig. 3.

If we take the subaperture testing without the alignment region 3 and auxiliary flat mirror, the testing CGH can be rotated anywhere around the focus, which means for a certain CGH, we cannot separate the position 1 and position 2 of the CGH in the subaperture testing as shown in Fig. 4.

By designing the alignment region 3 on CGH as shown in Table 1, the position 1 and position 2 in Fig. 4 can be distinguished by interference fringes corresponding to region 3. Considering the position 1 is the region to be tested, and the position 2 is the error region. After accomplishing the testing of the prior subaperture, by placing the CGH in the optical path, only the interference fringes formed with region 3 in the position 1 will be zero fringe pattern. If the testing subaperture is corresponding to the position 2 of relative CGH, there will be no zero fringe pattern formed with region 3.

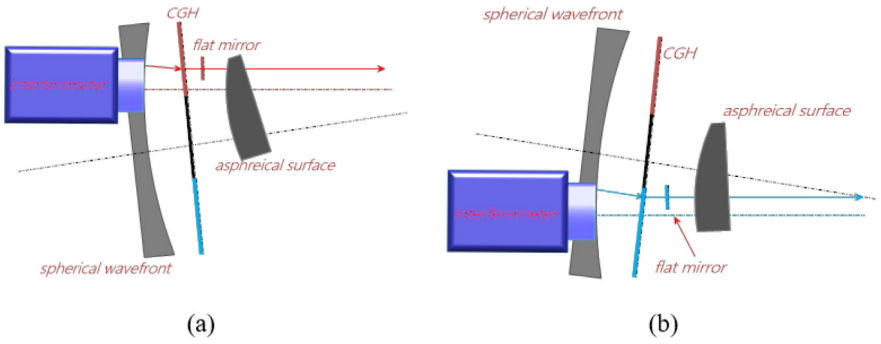

Fig. 3. Alignment between subapertures with auxiliary flat mirror . (For interpretation of the references to color in this figure legend, the reader is referred to the web version of this article.)

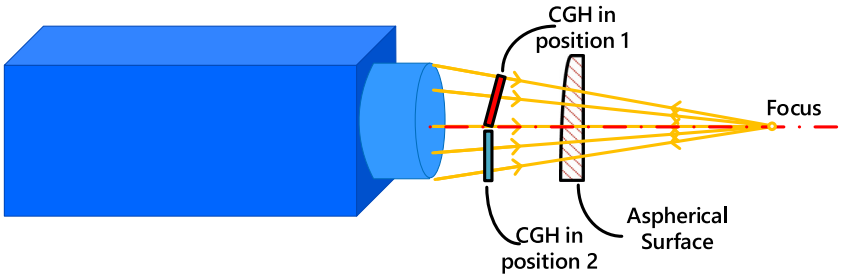

Fig. 4. CGH location relationship of different subapertures.

Based on the designed diffractive regions and auxiliary flat mirror, subapertures can be tested accurately and alignment between adjacent subapertures can be accomplished according to the following steps:

Step 1: Accomplish the null testing for the subaperture 1 of the aspherical surface as shown in Fig. 3(a) (The red CGH in Fig. 3(a) is adopted in this subaperture testing). In this step, the interferogram formed by region 2 on the CGH is null. After passing through region 3 on the CGH, the incident spherical wavefront is perpendicular to the auxiliary flat mirror. The relative surface map of subaperture 1 can be obtained with region 1 on the CGH.

Step 2: Keep the interferometer and the auxiliary flat mirror stationary, put the CGH of subaperture 2 in the optical path (the blue CGH in Fig. 3(b)). Then we adjust the position of the CGH, making the interferogram formed by region 2 on the CGH is null and the wavefront passing through region 3 on CGH is perpendicular to the auxiliary flat mirror. By adjusting the aspherical surface to the proper position, the surface map of subaperture 2 is obtained. With the above method, the relative positions between subaperture 1 and subaperture 2 is accurately aligned.

Step 3: Following the above steps until all subapertures are tested, the full aperture surface can be stitched with our proposed stitching algorithm described in Section 2.2.

2.2. Stitching algorithm

In order to obtain the full aperture map, we propose an iterative stitching algorithm to connect all the subaperture maps together [9]. In the stitching testing, N subapertures are measured in total, where the Nth subaperture is regarded as a reference subaperture. As a result, the testing map of the ith subaperture can be described as follows:

$$Z_i'(x,y) = Z_i(x,y) + \sum_{j=1}^{L} a_{ij} f_j(x,y) \tag{4}$$

where $Z_i(x,y)$ is the testing result of the ith subaperture, $f_j(x,y)$ is the alignment error terms between subapertures to be fitted, L is the number of alignment error terms, and a_{ij} is the relative fitted coefficient. In our compensating stitching testing, four polynomials including piston, tilt, tip and defocus are chosen as the alignment error terms. Based on Eq. (4), a merit function F is defined as follows,

$$F = \sum_{i=1\cdots N} \sum_{\substack{k=1\cdots N \\ k\neq i}}^{i\cap k} [(Z_i(x,y) + \sum_{j=1}^{L} a_{ij} f_j(x,y)) - (Z_k(x,y) + \sum_{j=1}^{L} a_{kj} f_j(x,y))]^2 \tag{5}$$

By minimizing the merit function F, a group of linear functions can be obtained as shown in Eq. (6).

$$\mathbf{P} = \mathbf{Q}\cdot\mathbf{R} \tag{6}$$

The vector $\mathbf{P}$, $\mathbf{R}$ and the matrix $\mathbf{Q}$ are defined as follows. For the observation vector $\mathbf{P}$, which is in length of $(N\text{-}1)\cdot L$ row, the element in the $((M-1)\cdot L + j)$th row can be described as follows,

$$P_{(M-1)\cdot j} = \sum_{M-1} \sum_{\substack{i=1 \\ i\neq(M-1)}}^{N} f_j(x,y)(Z_{(M-1)}(x,y) - Z_i(x,y))c_{i(M-1)}, \tag{7}$$

where

$$c_{ij} = \begin{cases} 1 & i\cap j \neq \varnothing \\ 0 & i\cap j = \varnothing \end{cases}. \tag{8}$$

For the data matrix $\mathbf{Q}$, which is a square matrix with $(N\text{-}1)\cdot L$ rows and $(N\text{-}1)\cdot L$ columns, the element in the $((M-1)\cdot L + j)$th row and $((H-1)\cdot L + k)$th column can be described as follows,

$$Q_{((M-1)\cdot j)((H-1)\cdot k)} = \begin{cases} -\sum_{(M-1)} \sum_{\substack{i=1 \\ i\neq(M-1)}}^{N} f_j(x,y)\cdot f_k(x,y)\cdot c_{i(M-1)} & M = H \\ \sum_{M-1}\sum_{H-1} f_j(x,y)\cdot f_k(x,y)\cdot c_{(M-1)(H-1)} & M \neq H \end{cases}. \tag{9}$$

Then the coefficients vector $\mathbf{R}$ can be calculated. The element in the $((M-1)\cdot L + j)$th row of vector $\mathbf{R}$ can be expressed as follows,

$$R_{(M-1)\cdot j} = a_{(M-1)j} \tag{10}$$

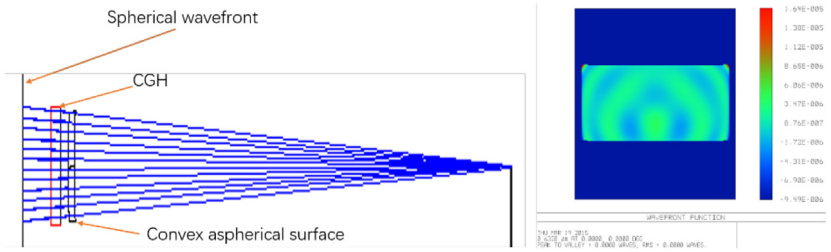

Fig. 5. Full aperture compensation design result. (a) optical path for CGH compensating testing in full aperture; (b) design residual result.

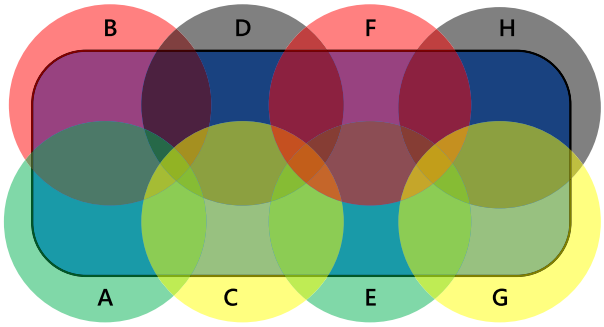

Fig. 6. Sub-CGHs design.

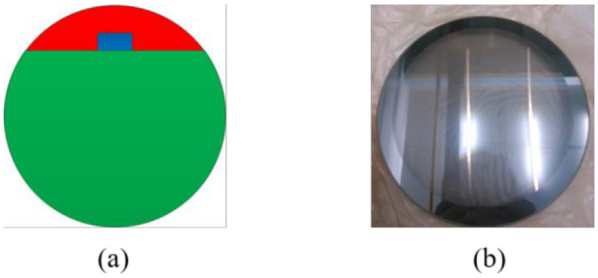

Fig. 7. CGH in the experiment: (a) diffractive regions distribution on CGH; (b) one of the CGH used in the measurement.

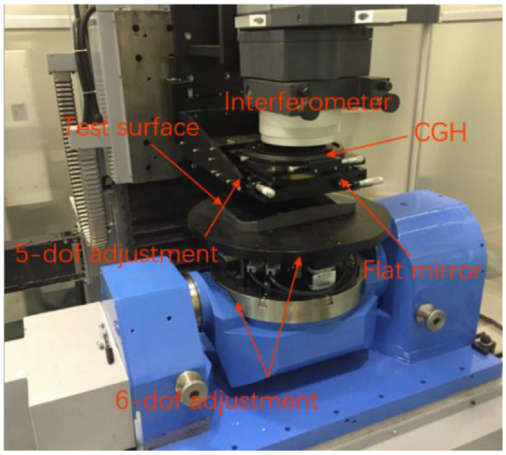

Fig. 8. Experimental setup.

After calculating the relative alignment coefficients between subapertures with Eqs. (4)–(10), the alignment errors can be removed from each subaperture. Then by connecting all the subapertures together, the full aperture map is reconstructed.

3. Experiment verification

To evaluate the performance of our proposed method, experimental verification was conducted by testing an off-axis convex aspherical surface with its aperture of 332 mm×144 mm, whose peak to valley (PV) aspherical departure can be about 132.4λ (λ = 632.8 nm). The radius of curvature at the apex of the aspherical surface is -933 mm and the conic constant κ is −0.54. The off-axis amount of the aspherical mirror is 86.2 mm.

If we apply stitching testing to this aspherical surface directly and limit the departure in each subaperture within 5λ (λ = 632.8 nm), the diameter of each subaperture will be less than 40 mm. Therefore, to accomplish the full aperture coverage of the aspherical surface, more than fifty subapertures are necessitated. Since each subaperture is relatively small to achieve full aperture coverage, the required number of subapertures is so many that it is very difficult to remove the retrace error in the non-null testing of each subaperture [24,25]. As a result, it is untoward to obtain a stitching result with satisfactory accuracy.

To improve reconstruction accuracy of the full aperture surface, we combine stitching testing with CGH compensating testing. The full aperture CGH compensating optical path is shown in Fig. 5(a) and relative design residual result is shown in Fig. 5(b).

The full aperture size of the CGH is 354 mm×150 mm, while the PV and RMS of the design residual result are both zero. Since the aperture of the interferometer is 150 mm, eight pieces of CGH are designed to accomplish the full aperture coverage of the aspherical surface as shown in Fig. 6.

Based on the theory described in Section 2.1.2, to achieve accurate alignment between subapertures, three kinds of diffractive region including two alignment regions are designed on each CGH as shown in Fig. 7(a) and one of the fabricated CGH used in the measurement is shown in Fig. 7(b).

As shown in Fig. 7(a), the green region is the compensation region for the testing of each subaperture, the red region is used to accomplish the alignment between the CGH and the interferometer, and the blue region is designed to realize the alignment between the CGH and the auxiliary flat mirror. The experiment setup is shown in Fig. 8.

In the experiment, a laser Fizeau interferometer with a 150 mm diameter reference optics was set up for the subaperture testing and the relative eight subaperture testing results are shown in Fig. 9.

Applying our proposed stitching algorithm to the testing results of all subapertures shown in Fig. 9, the full aperture map can be obtained as shown in Fig. 10. The PV and RMS values of the stitching map are 0.639λ and 0.069λ respectively (λ = 632.8 nm).

In consideration of cross validation, the off-axis convex aspherical surface was also tested with hybrid compensation method as shown in Fig. 11 [26]. In the testing, a spherical mirror in 750 mm aperture and a CGH are introduced to realize the null testing of the aspherical surface.

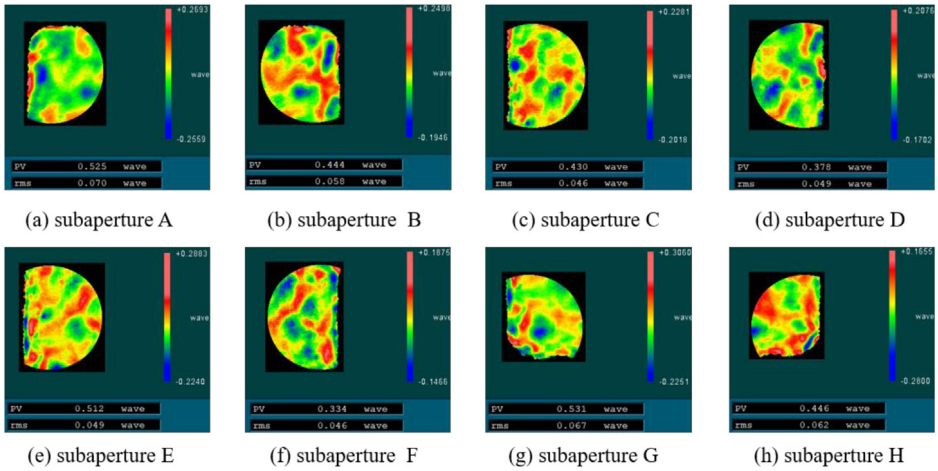

Fig. 9. Testing results of all subapertures.

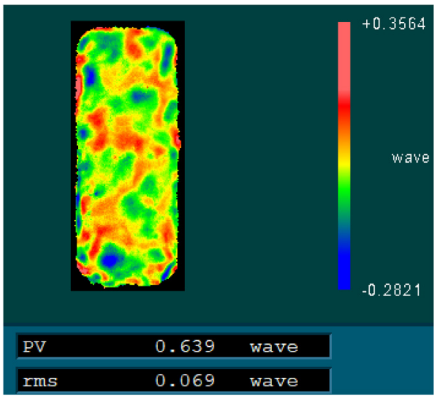

Fig. 10. Stitching map result.

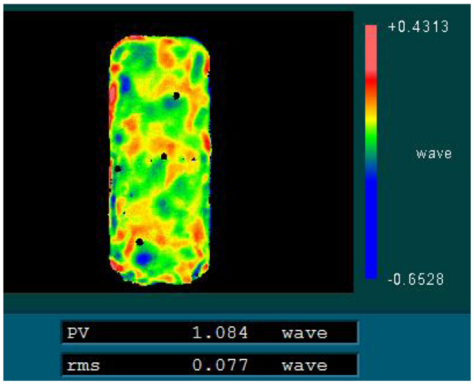

Fig. 12. Testing map from hybrid compensation method.

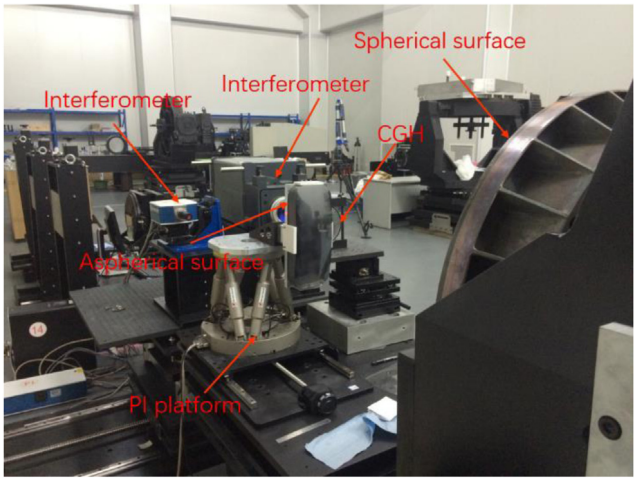

Fig. 11. Experimental setup for hybrid compensation method.

The spherical surface can be used to compensate the main aberrations, and the residual aberrations can be compensated by the CGH. The relative aspherical surface testing result is shown in Fig. 12. The PV and RMS values of the testing map are 1.084λ and 0.077λ respectively (λ = 632.8 nm). By comparing Figs. 10 and 12, the surface error distribution obtained by two methods are consistent, which verifies the accuracy and availability of our compensating stitching method.

As both the above methods can be adopted to reconstruct the full aperture map of the testing aspherical surface, our proposed compensating stitching method is relatively more advantageous compared with the hybrid compensation method as shown in Fig. 11 from the following aspects. Firstly, our method avoids the necessity of a large aperture spherical mirror, which may be difficult to fabricate in the testing. Secondly, for the hybrid compensation method, spherical surface error will be added in the aspherical testing map, and complex calibration and calculation are required to remove the error in this process. Thirdly, five components including two interferometers, CGH, spherical mirror and convex aspherical mirror are required in the testing optical path of the hybrid compensation method, which makes the accurate alignment between optics more complicated, and the non-alignment between optics will introduce extra aberrations in the aspherical testing map. Honestly, for our compensating stitching method, multiple CGHs and measurements are needed and therefore it takes more time in the testing. Nevertheless, our compensating stitching method provides an alternative approach for convex aspherical surface testing. Since the CGH has more degrees of freedom in design, our proposed method can be more powerful in testing more complex surfaces, such as off-axis high-order aspherical surfaces and even freeform surfaces.

4. Conclusion

We have provided a compensating stitching method to test convex aspherical surfaces. In the testing, relative CGH is designed for each programmed subaperture and null testing is applied in each subaperture testing. To avoid misalignment between subapertures, specialized

alignment region is designed on each CGH and an auxiliary flat mirror is introduced to accomplish accurate alignment between subapertures. To evaluate the performance of our compensating stitching method, experimental verification was conducted by testing an off-axis convex aspherical surface. Our experimental results demonstrate that our proposed method can obtain the reconstructed surface map in full aperture with satisfactory accuracy. We can confidently conclude that our compensating stitching method can help accomplish the full aperture testing for convex aspherical surfaces with large departure.

Declaration of competing interest

The authors declare that they have no known competing financial interests or personal relationships that could have appeared to influence the work reported in this paper.

Funding

National Natural Science Foundation of China (61805089 and 61805088); the Fundamental Research Funds for the Central Universities (2018KFYYXJJ053, 2019kfyXKJC040, and 2019kfyRCPY083).

References

[1] C.J. Kim, Polynomial fit of interferograms, Appl. Opt. 21 (24) (1982) 4521–4525.
[2] J.G. Negro, Subaperture optical system testing, Appl. Opt. 23 (24) (1982) 4521–4525.
[3] C.J. Kim, J.C. Wyant, Subaperture test of a large flat or a fast aspheric surface, J. Opt. Soc. Amer. 71 (1981) 1587.
[4] Y.F. Wen, H.B. Cheng, Hon-Yuen Tam, D.M. Zhou, Modified stitching algorithm for annular subaperture stitching interferometry for aspheric surfaces, Appl. Opt. 52 (23) (2013) 5686–5694.
[5] X. Hou, F. Wu, L. Yang, Q. Chen, Experimental study on measurement of aspheric surface shape with complementary annular subaperture interferometric method, Opt. Express 15 (20) (2007) 12890–12899.
[6] L.S. Yan, D.Y. Zhu, X.K. Wang, M. Li, X.F. Zeng, D.L. Ma, Measurement of rotationally symmetric aspherical surfaces with the annular subaperture stitching mthod, Appl. Opt. 58 (26) (2019) 7073–7079.
[7] S.Y. Chen, S. Xue, Y.Y. Dai, S.Y. Li, Subaperture stitching test of large steep convex spheres, Opt. Express 23 (22) (2015) 29047–29058.
[8] Z.X. Zhao, H. Zhao, F.F. Gu, H.B. Du, K.X. Li, Non-null testing for aspheric surfaces using elliptical sub-aperture stitching technique, Opt. Express 22 (5) (2014) 5512–5520.
[9] L.S. Yan, X.K. Wang, L.G. Zheng, X.F. Zeng, H.X. Hu, X.J. Zhang, Experimental study on subaperture testing with iterative triangulation algorithm, Opt. Express 21 (19) (2013) 22628–22644.
[10] L. Zhang, D. Liu, T. Shi, Y.Y. Yang, S.Y. Chong, B.L. Ge, Y.B. Shen, J. Bai, Aspheric subaperture stitching based on system modeling, Opt. Express 23 (15) (2015) 19176–19188.
[11] O. Masashi, O. Katsuyuki, T. Jumper, Measurement of large plane surface shapes by connecting small-aperture interferograms, Opt. Eng. 33 (20) (1994) 608–613.
[12] C. Tian, Y.Y. Yang, T. Wei, Y.M. Zhuo, Nonnull interferometer simulation for aspheric testing based on ray tracing, Appl. Opt. 50 (20) (2011) 3559–3569.
[13] Y.C. Chen, C.W. Liang, H.S. Chang, P.C. Lin, Reconstruction of reference error in high overlapping density subaperture stitching interferometry, Opt. Express 26 (22) (2018) 29123–29133.
[14] S.Y. Chen, S. Xue, G.L. Wang, Y. Tian, Subaperture stitching algorithms: A comparision, Opt. Commun. 390 (2017) 61–71.
[15] P.F. Zhang, H. Zhao, X. Zhou, J.J. Li, Subaperture stitching interferometry using stereovision positioning technique, Opt. Express 18 (14) (2010) 15216–15222.
[16] J.G. Thunen, O.Y. Kwon, Full aperture testing with subaperture test optics, Proc. SPIE 351 (1982) 19–27.
[17] W.W. Chow, G.N. Lawrence, Method for subaperture testing interferogram reduction, Opt. Lett 8 (1983) 468–470.
[18] T.W. Stuhlinger, Subaperture optical testing: experimental verification, Proc. SPIE 656 (1986) 118–127.
[19] P. Su, J.H. Burge, R.E. Parks, Application of maximum likelihood reconstruction of subaperture data for measurement of large flat mirrors, Appl. Opt. 49 (1) (2010) 21–31.
[20] Z.M. Yang, J.U. Du, C. Tian, J.T. Dou, Q. Yuan, Z.S. Gao, Generalized shift-rotation absolute measurement method for high-numerical-aperture spherical surfaces with global optimized wavefront reconstruction algorithm, Opt. Express 25 (21) (2017) 26133–26147.
[21] A. Kulawiec, P. Murphy, M.D. Marco, Measurement of high-departure aspheres using subaperture stitching with the Variable Optical Null (VON™), Proc. SPIE 7655 (2010) 765512.
[22] C. Supranowitz, C.M. Fee, P. Murphy, G. Forbes, A. Kulawiec, D. Miladinovic, Asphere metrology using variable optical null technology, Proc. SPIE 8416 (2012) 841604.
[23] Wenru Cai, Wavefront Analysis and Calibration for Computer Generated Holograms (Doctor thesis), The university of Arizona, 2013.
[24] C. Tian, Y.Y. Yang, T. Wei, Y.M. Zhuo, Nonnull interferometer simulation for aspheric testing based on ray tracing, Appl. Opt. 50 (20) (2011) 3559–3569.
[25] D. Liu, Y.Y. Yang, C. Tian, Y.J. Luo, L. Wang, Practical methods for retrace error correction in nonnull aspheric testing, Opt. Express 17 (9) (2009) 7025–7035.
[26] L.S. Yan, D.Y. Zhu, X.F. Zeng, M. Li, X.K. Wang, D.L. Ma, Experimental study on hybrid compensation testing of an off-axis convex ellipsoid surface, Opt. Express 27 (20) (2019) 27546–27561.